

Chapter 7: Remotely sensed rain and snowfall in the Himalaya

Taylor Smith and Bodo Bookhagen

Institute of Earth- and Environmental Science, University of Potsdam, Karl-Liebknecht-Str. 24/25, 14467 Potsdam-Golm, Germany

Abstract

Waters sourced in the Himalaya flow through the Ganges and Indus basins, which are some of the most densely populated regions of the world. Both communities in the mountains and those downstream are highly dependent on the volume and consistency of runoff. A growing body of research has pointed towards changes in the timing, volume, and spatial distribution of precipitation in the region over the past decades, but our understanding of the magnitude and direction of these trends is limited by lack of in-situ data availability, complex terrain, and poor process understanding.

Remote sensing provides long-term and spatially-extensive climate data over the entire Himalayan region, and allow for detailed analysis of large-scale environmental change. Here we use several complimentary datasets to explore recent changes in both liquid and solid precipitation, and the knock-on impacts on the Himalayan cryosphere. We find that the spatial and temporal distribution of water resources has shifted, with potentially significant consequences for downstream water provision. In particular, we find that there has been less water stored in snowpack over the past decades, and that the timing of the snowmelt season has shifted earlier in the year. The length of the snowmelt season has also been compressed in much of the region. Rainfall trends can also be detected in the time series, however, multi-annual oscillations and intra-seasonal variations make it difficult to obtain statistically significant trends. Continued exploration of these time series and their associated trends will be essential for understanding hydro-meteorologic processes and improving future regional water planning.

Introduction

More than a billion people rely on water sourced in the Himalayan region for hydropower, agriculture, and household water resources (Bolch et al., 2012; Immerzeel et al., 2010). Both small and large communities are often highly dependent on the consistency of precipitation; many lack the resources to respond to rapid changes in water availability. Over the past decades, significant changes in the hydrological cycle of the Himalaya have been observed.

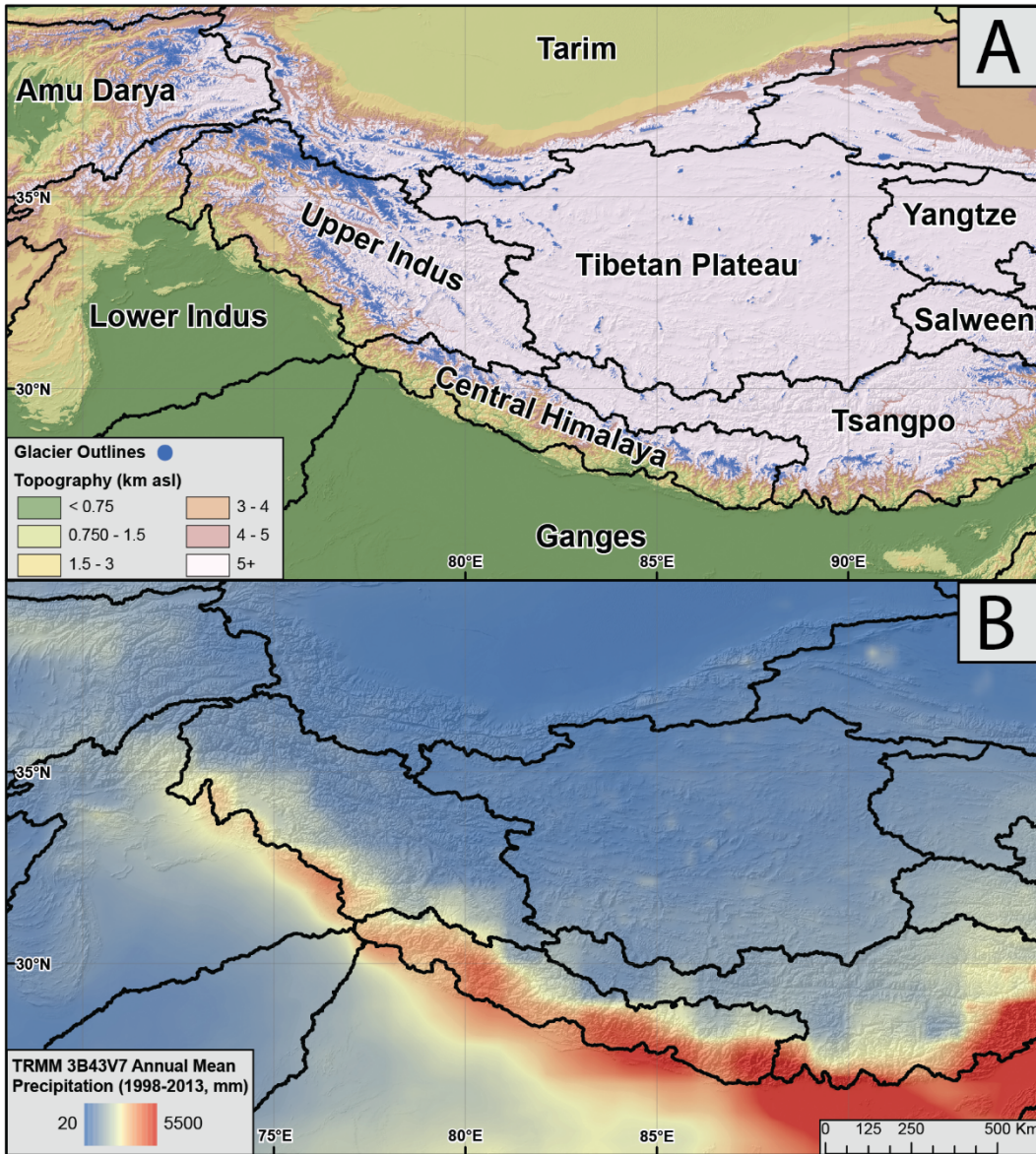


Figure 1 – (A) Topography of the Himalaya region, showing major watershed boundaries and glacier outlines in blue based on the Randolph Glacier Inventory (V6) (RGI Consortium, 2017). (B) Mean annual Tropical Rainfall Measurement Mission (TRMM) 3B43 rainfall (Huffman et al., 2007), showing distinctive precipitation gradient along and across strike (cf. Bookhagen and Burbank, 2010).

The study region runs from 25-40 N and 65-95 E, covering several large and glaciated watersheds (0A). There exists a distinct precipitation gradient from east to west and north to south, which generally follows the track of the Indian Summer Monsoon (ISM) along the front of the Himalaya (0B, cf. Bookhagen and Burbank, 2010). Large regions of the Himalaya, particularly those above 4,000 m asl, also receive significant amounts of precipitation in the form of snow throughout the year (0).

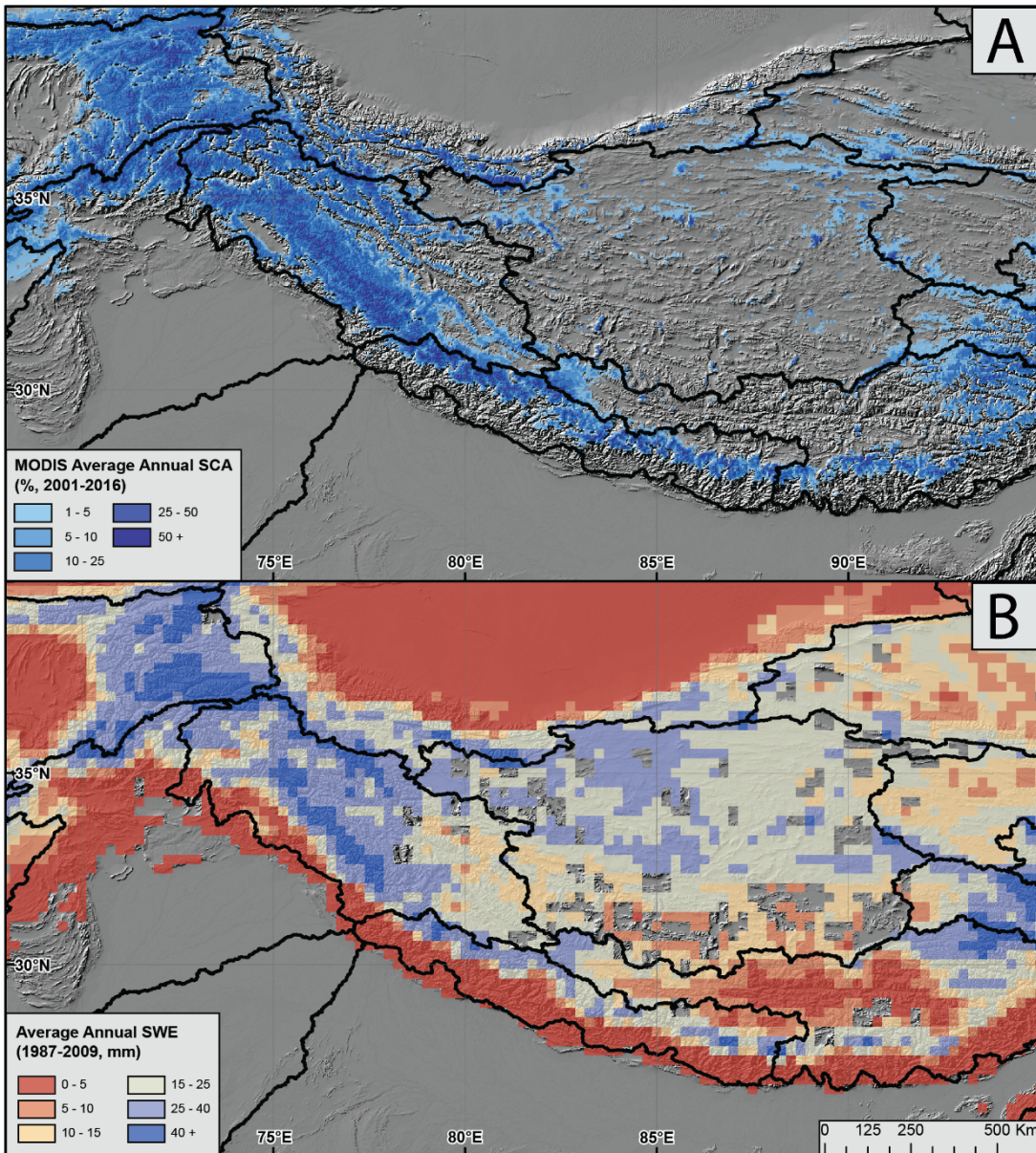


Figure 2 – (A) Moderate Resolution Imaging Spectroradiometer (MODIS) average annual snow covered area (Hall et al., 2006), showing distinctly higher snow cover in the west and at high elevations. (B) Average annual Snow-Water Equivalent (SWE) from Special Sensor Microwave/Imager (SSMI) data (1987-2009), showing similar but not identical spatial patterns (for data processing information see Smith and Bookhagen, 2018). The largest snow-water volumes are stored in the western regions of the Himalaya.

In the eastern regions of the Himalaya, there is significantly more rainfall than snowfall. The western reaches of the Himalaya, however, receive a large percentage of their water budget in the form of snow, particularly in the coldest regions of the Himalaya (0). The western parts of the Himalaya are generally colder than the eastern regions, and maintain much larger concentrations of glaciers (cf. 0A, blue regions). However, there exists a very high elevation band – along the highest peaks of the world – that is well below freezing for much of the year and receives significant snowfall.

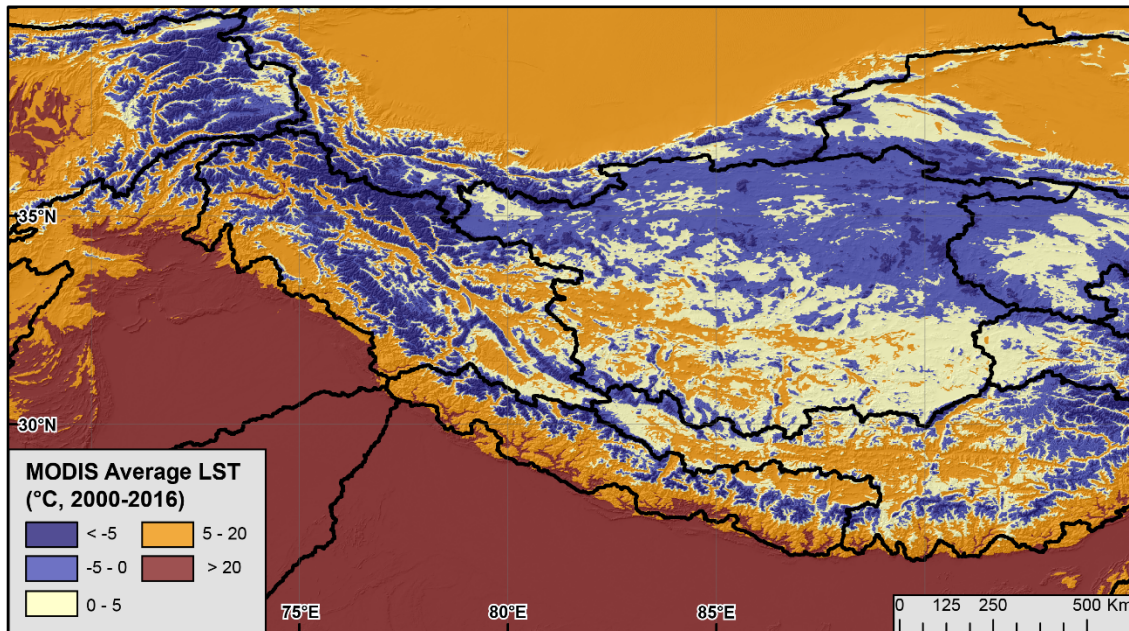


Figure 3 – MODIS average annual land-surface temperature (LST, product MOD11A2 V006, Wan et al., 2015). Significant regions of the Himalaya maintain average annual temperatures well below zero.

Throughout the region, and in particular in the very cold parts of the study area, snow remains on the ground through a large portion of the year (0). These snow-covered regions are not confined to areas surrounding glaciers, but also extend into the high Tibetan Plateau – although this snow-cover is often quite shallow.

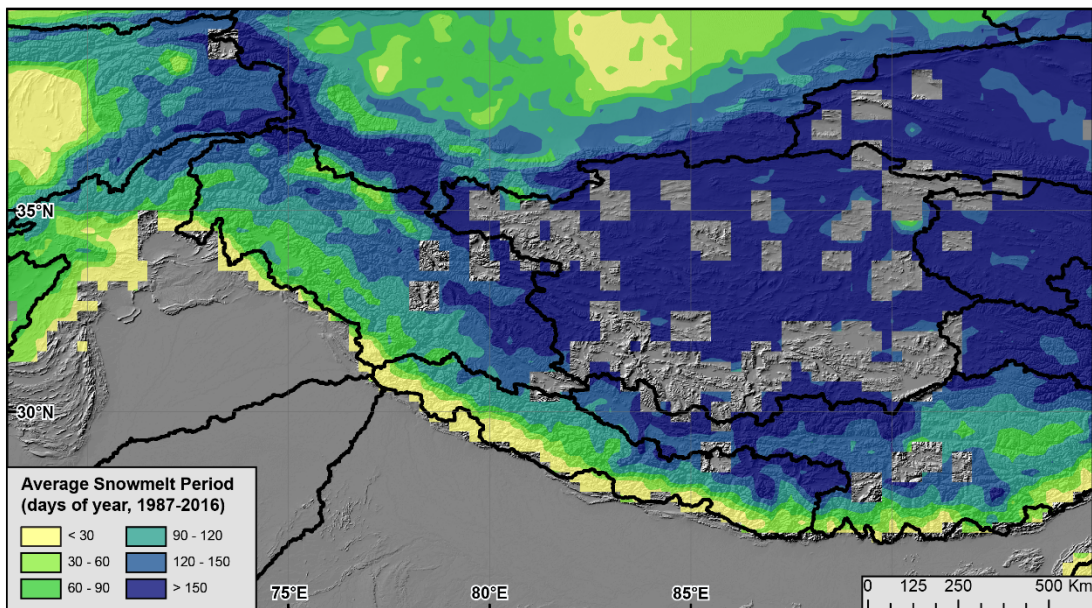


Figure 4 – Average annual snowmelt period based on passive microwave data (modified after Smith et al., 2017). Cold regions, particularly around the highest peaks and through the central Tibetan Plateau, maintain at least sparse snow cover for large portions of the year.

Recent Climate Changes in the Himalaya

There have been substantial changes in the regional climate, including increased temperatures (Vaughan et al., 2013), increased storm intensity (Singh et al., 2014; Yao et al., 2012; Bookhagen and Burbank, 2010; Malik et al., 2016; Fu, 2013; Palazzi et al., 2013), changes in the ISM (Gautam et al., 2009; Menon et al., 2013; Kitoh et al., 2013),

intensification of the Winter Westerly Disturbances (WWD) (Cannon et al., 2014; 2015), and substantial changes in glaciers throughout the region (Bolch et al., 2012; Kääb et al., 2014; 2015; Kapnick et al., 2014; Gardner et al., 2013; Yao et al., 2012; Gardelle et al., 2012; Scherler et al., 2011; Frey et al., 2014).

The shrinking of Himalayan glaciers over the past decades is a highly visible sign of regional climate change (Bolch et al. 2012). As water stored in these glaciers is an important part of the hydrological budget of many Himalayan catchments, any changes in glacier water storage capacity will have significant downstream impacts (Vaughan et al., 2013). Historically, water has been slowly released from snow and glaciers throughout the spring and summer, providing year-round water to both high-elevation and downstream communities. However, recent climate changes have reduced the dependability of the yearly hydrological cycle. Many regions have seen increases in early season runoff alongside drastic decreases in late season runoff – particularly in those regions where glaciers have substantially retreated or disappeared (Lutz et al., 2014). The Intergovernmental Panel on Climate Change (IPCC) forecasts that runoff in major river basins of the Himalaya will increase through 2100 due to both changes in glaciers and large-scale precipitation patterns, and then decrease after the end of the century (Vaughan et al., 2013). However, these large-scale changes conceal regional, small-scale, and seasonal variation in climate change impacts which are already being felt in the region.

Recent work has noted that the spatial and temporal patterns of snow-water storage have shifted over the past decades (Smith et al., 2017; Smith and Bookhagen, 2018). In many regions, snow-water storage has peaked earlier in the year, and melted more rapidly during the spring (Smith et al., 2017). Annual trends in snow-water storage throughout the region are also majority negative, implying that changes in temperature and precipitation patterns have already had strong impacts on the cryosphere (Immerzeel et al., 2010; 2012; Smith and Bookhagen, 2018). As snow meltwaters account for a large portion of many hydrological budgets, any changes in the magnitude and timing of snowmelt will have significant downstream impacts.

Large-scale climate patterns -- such as the ISM and WWD -- have changed in strength and timing (e.g., Cannon et al., 2014; 2015; Gautam et al., 2009; Menon et al., 2013; Kitoh et al., 2013; Fu, 2003; Palazzi et al., 2013; Ramanathan et al., 2005; Lau et al. 2010). For example, the ISM has increased in strength since the 1950s due to increases in moisture availability (Menon et al., 2013; Kitoh et al., 2013) and increased regional heat-trapping potential due to air pollution (Ramanathan et al., 2005; Lau et al. 2010). In addition to climate change, shifts in Southeast Asia's landcover (i.e., deforestation, extensive irrigation and agriculture, urbanization) have modified regional weather and climate patterns (Fu, 2003; Gautam et al., 2009; Bookhagen and Burbank, 2010). Large-scale changes in ENSO patterns due to warming oceans have also impacted precipitation patterns in the Himalaya (Bookhagen et al., 2005).

Satellite datasets, such as the Tropical Rainfall Measurement Mission (TRMM) (Huffman et al., 2007) and modeling efforts, such as High Asia Refined Analysis (Maussion et al., 2014) and Asian Precipitation - Highly-Resolved Observational Data Integration Towards Evaluation (APHRODITE) (Yatagai et al., 2012), rarely agree on the magnitude and direction of changes in temperature and precipitation (Malik et al., 2016), and have trouble correctly quantifying high-elevation precipitation (Li et al., 2017; Immerzeel et al., 2015). A lack of long-term and spatially extensive in-situ empirical observations (0) limits our process understanding (Bookhagen and Burbank, 2010; Sorg et al., 2012), and leads to large disagreements in climate projections in global and regional models (Kapnick et al., 2014; Vaughan et al., 2013).

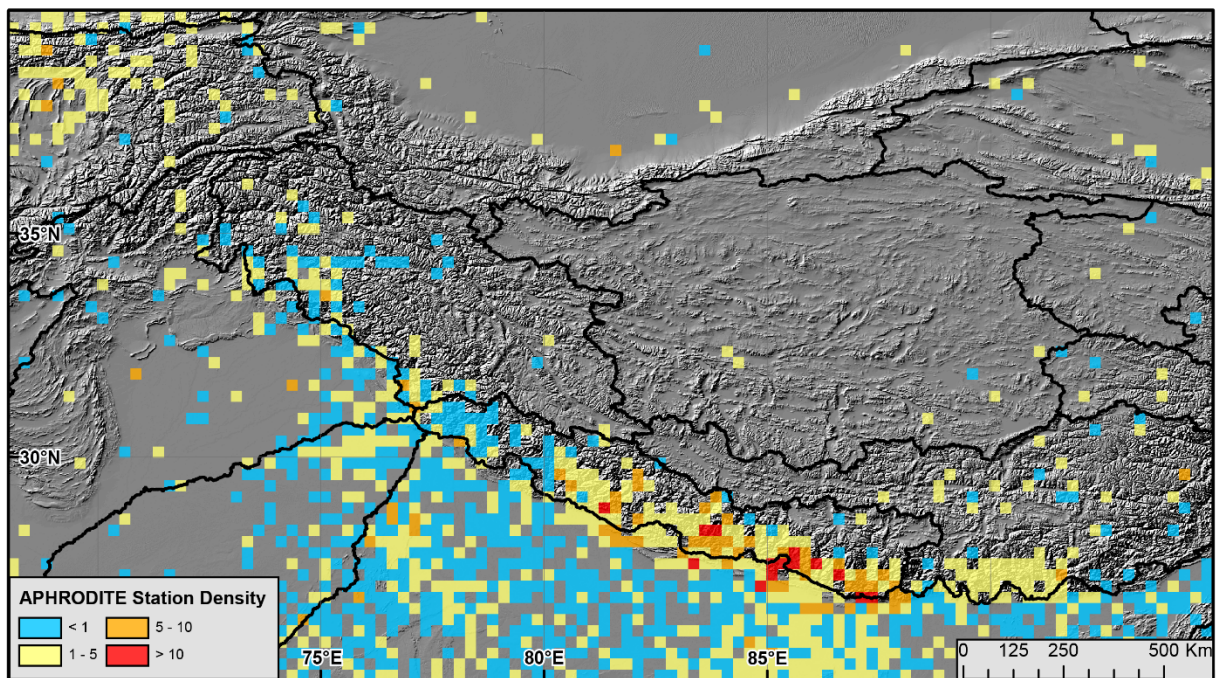


Figure 5 – APHRODITE climate station density (1961-2007) (Yatagai et al., 2012, figure modified after Smith and Bookhagen, 2018). While parts of the Himalayan foreland are well monitored, much of the Tibetan interior lacks in-situ climate measurements. The majority of these stations measure rainfall and temperature, and very few measure snow depth or snow-water equivalent.

While satellite datasets each have their own strengths and weaknesses, they provide the only long-term, spatially continuous, empirical set of observations of the remote and rugged Himalayan region. Several different satellite platforms have been used to great effect in the Himalaya, and provide optical, active radar, passive microwave, gravimetry, and precipitation measurements across the entire region with high temporal frequency. This chapter explores changes in rain and snowfall in the Himalaya using a set of complimentary remote sensing datasets.

Data and Methods

Rainfall data are derived from the TRMM product 3B42 (Huffman et al., 2007), at a 3-hour temporal resolution. The spatial resolution of this data is $0.25^\circ \times 0.25^\circ$ ($\sim 25 \times 25 \text{ km}^2$), with data available from 1998 to 2014. As short-duration storms may be missed during satellite overpasses, we aggregate data here to daily and monthly means before performing precipitation analyses.

The Moderate Resolution Imaging Spectroradiometer (MODIS) land-surface temperature (LST) product MOD11A2 (V006) dataset was used to explore regional temperature (Wan et al., 2015). The data has an 8-day temporal frequency and a 1-km spatial resolution. In this study, we use data from 2000 until 2017. We also leverage MODIS maximum mean monthly snow cover (product MOD10C1, V005) at $0.05^\circ \times 0.05^\circ$ ($\sim 5 \times 5 \text{ km}^2$) spatial resolution over the same study period (Hall et al., 2006).

We use reprocessed Satellite Pour l'Observation de la Terre (SPOT) data from 1998-2014 (product VGT-S10, Deronde et al., 2014) to generate long-term average normalized difference vegetation index (NDVI) values. This data has a 10-day temporal and 1-km spatial resolution.

Several passive microwave sensors were used to examine changes in snow-water storage and snowmelt timing. The five sensors used are the Special Sensor Microwave/Imager (SSMI, 1987-2009) (Wentz, 2013), Special Sensor Microwave Imager/Sounder (SSMIS, 2003-2017) (Sun and Weng, 2008), Advanced Microwave Scanning Radiometer – Earth Observing System (AMSR-E, 2002-2011) (Ashcroft and Wentz, 2013), AMSR2 (2012-2017) (Imaoka et al. 2010) and the Global Precipitation Measurement Core Observatory (GPM, 2014-2017) (GPM Science Team, 2014). These satellites each carry slightly different microwave frequencies, but can each be used to derive snow properties.

Snow-water equivalent (SWE) is derived from the passive microwave data using the Chang equation (Chang et al., 1987), with modifications for non-SSMI platforms as proposed by Armstrong and Brodzik (2001), and a constant snow density of 0.24 g/cm^3 as proposed by Takala et al. (2011). This data is used to both derive annual and seasonal trends (after Smith and Bookhagen, 2018) and to assess changes in the timing and length of the snowmelt season (after Smith et al., 2017). For a more detailed discussion of passive microwave data processing methodologies, please see Smith and Bookhagen (2018), Smith et al. (2017), and Smith and Bookhagen (2016).

Results

Along and across-strike rainfall gradients

There exists a clear rainfall gradient running from east to west along the front of the Himalaya (cf. 0). This precipitation gradient also engenders a vegetation gradient (0). In particular, the interior of the Tibetan Plateau is sparsely vegetated, especially at high elevations and in the west. In addition to the along-strike gradients, there exist clear differences in the across-strike topographic and precipitation patterns throughout the Himalaya.

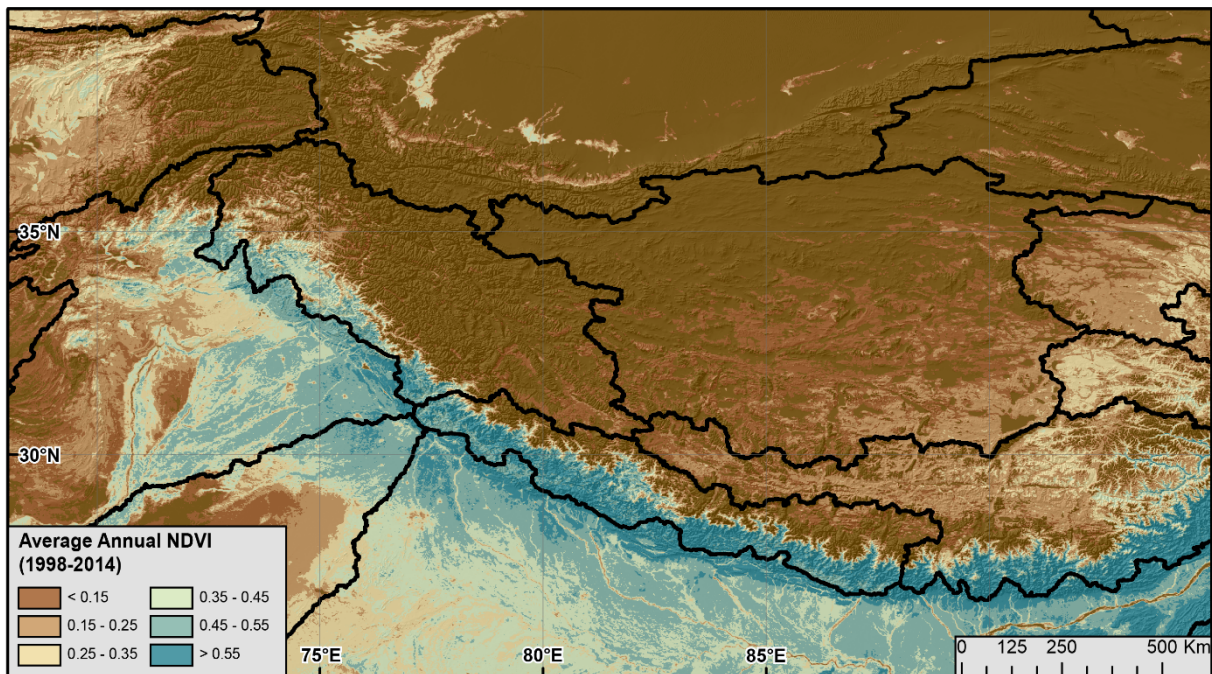


Figure 6 – Annual average NDVI values (1998-2014), from the SPOT (VGT-S10) dataset (Deronde et al., 2014). There exists a gradient running from denser vegetation in the east to sparse vegetation in the west and in the Tibetan interior (cf. Olen et al., 2016).

In the eastern and western reaches of the Himalaya, along the syntaxes (cf. 0A), topography rises smoothly towards 5,000 m asl. Precipitation mirrors this smooth rise with a single precipitation maximum along the topographic break. In the central portion of the Himalaya, however, there are two topographic steps, along the lesser and greater Himalaya (cf. 0B). These correspond to two distinct rainfall peaks – one at each topographic break.

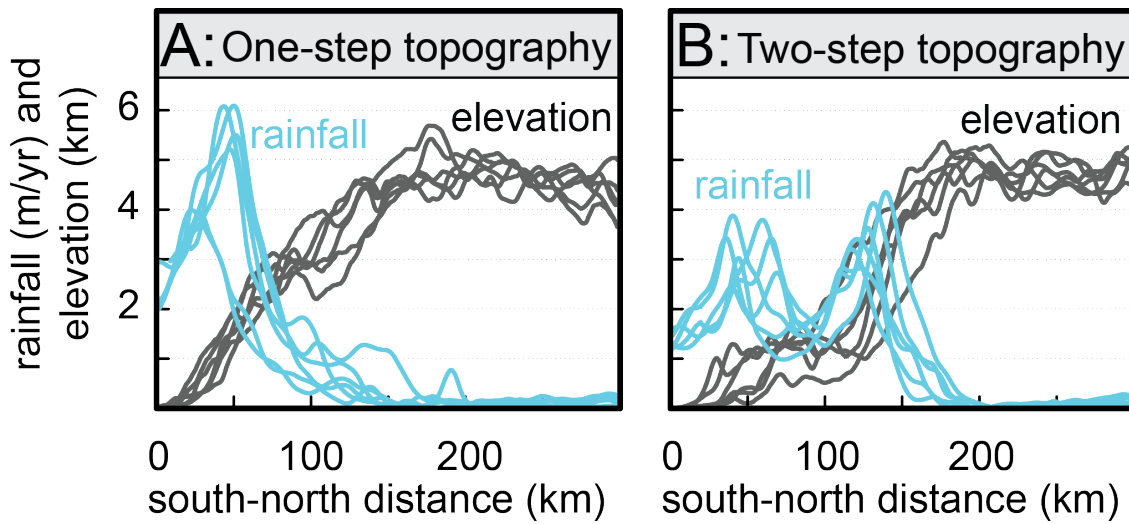


Figure 7 – Rainfall and elevation profiles perpendicular to the strike of the Himalaya in the (A) western and eastern ends and (B) central portion of the study area. The edges have a single topographic step and rainfall peak, whereas the central Himalaya has two topographic breaks and rainfall peaks. Modified from Bookhagen and Burbank, 2010.

Along-strike snow and glacier distribution

The distribution of snow-water resources also follows a similar east-west pattern (cf. 0). In particular, there is more extensive snow cover in the western regions of the Himalaya, and higher SWE storage. There is also significantly more glaciated area in the west (cf. 0). This can be easily seen when examining the aggregated snow, glacier, and topographic profiles of three catchments moving from west to east (0). Both the spatial and elevation distributions of snow change along this east-west gradient. While the general topographic distribution of the three examined catchments (Upper Indus, Central Himalaya, Tsangpo) remains similar, snow and glaciers occur at distinctly higher elevations moving towards the east.

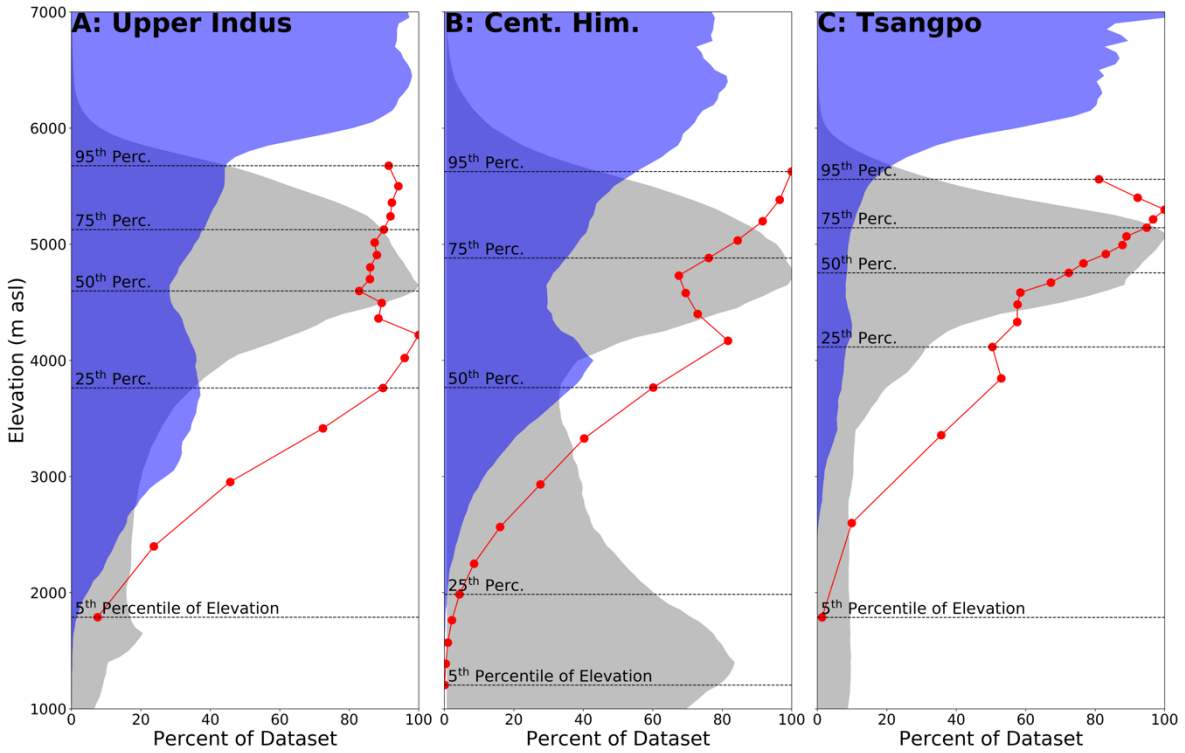


Figure 8 – (A) Upper Indus, (B) Central Himalaya, and (C) Tsangpo catchment hypsometries (grey), percentage glaciated area (blue) and normalized SWE distribution (red). All three values displayed as percentage of dataset maximum. While all three catchments have similar elevation distributions, SWE is stored at generally higher elevations moving from west to east. Modified after Smith and Bookhagen, 2018.

Along-strike climate analysis

In order to examine east-west climate and glacier coverage gradients, we construct a swath profile running along the length of the Himalaya from the Indus catchment through to the Tsangpo (0). We focus on areas along the main Himalayan arc, above 500 m asl. We find that maximal elevations along strike of the Himalaya remain roughly equivalent, at around 6,000 to 8,000 m asl, but that the area above 5,000 m asl varies significantly. There exist clear opposing east-west trends in frozen and liquid precipitation, where the eastern regions receive more rainfall and the western regions maintain higher SWE and snow-covered area. This is also reflected in the atmospheric lapse rate, which increases from (negative) 5 – 6 °C/km in the east to (negative) 3.5 – 4.5 °C/km in the west. We measure the lapse rate here not vertically in the atmosphere but along a N-S swath from the low-elevation foreland to the high-elevation Himalaya. The eastern Himalaya have a lower lapse rate than the western regions – particularly during the monsoon season – due to the relatively smaller temperature difference between the foreland and high-elevation areas. Further west, however, there exist much larger temperature gradients between the warmer foreland and extremely cold high-elevation zones. This effect is particularly strong during the winter months.

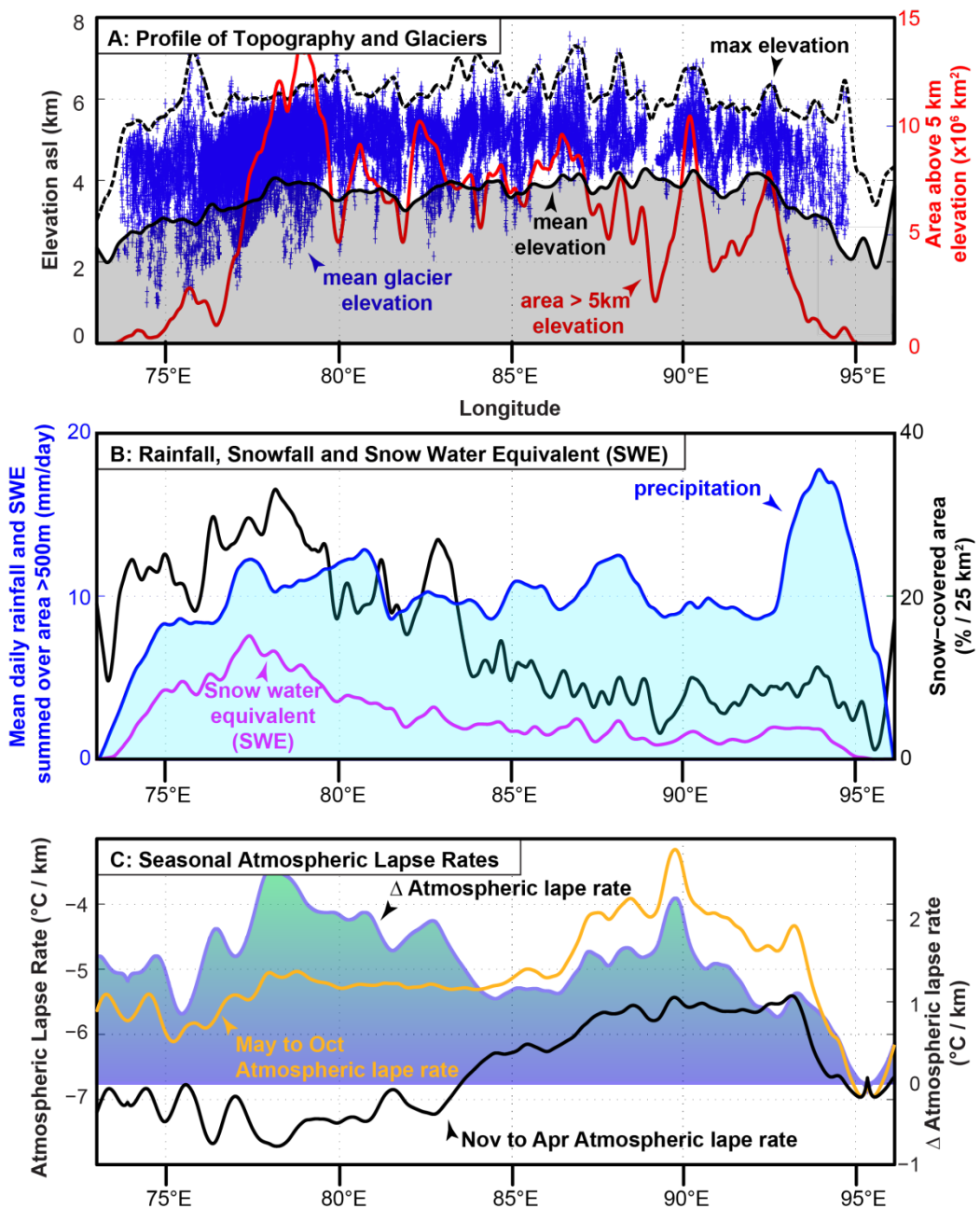


Figure 9 – West-to-east swaths with averaged profiles showing topography, climate, and atmospheric lapse rates (modified from Bookhagen, 2017), with values averaged north-to-south perpendicular to the strike of the Himalaya. (A) Maximal (black dashed) and mean (black solid) elevation, and area above 5,000 m asl. Blue crosses represent mean glacier elevation. (B) TRMM 3B42-derived precipitation (blue), SSMI SWE (purple) and MODIS snow-covered area (black). These profiles show strong west-east gradients, with more snow in the western reaches of the Himalaya. (C) Atmospheric lapse rates (summer, gold; winter, black; annual, shaded). Lapse rates in the eastern Himalaya have higher negative values during the summer due to the heating of the Tibetan Plateau and the increase of the temperature gradient.

Discussion

Spatial and temporal patterns of rainfall changes in the Himalaya

The spatial east-west rainfall gradient has been used in previous research to explain differences in sediment fluxes and erosion (Olen et al., 2016; Thiede et al., 2009; Dey et al., 2006; Hirschmiller et al., 2014). Similarly, the north-south rainfall gradient and the strike-parallel bands of orographic rainfall (cf. 0) have been used to explain spatially-focused erosion and landslide activity (e.g., Bookhagen et al., 2005). Recent research also has investigated the

differences in rainfall dynamics between areas of high annual precipitation (orographic rainfall) and regions in the luv and lee of the rainfall bands (e.g., Wulf et al., 2016). Time series analysis shows that rainfall magnitude-frequency distributions differ significantly on short spatial distances.

Rainfall during the monsoon season is the main driver of hydrological processes in the central Himalaya and contributes significantly to the annual precipitation budget. In most parts of the central Himalaya, rainfall during the monsoon season – between June and September – contributes on average more than 80% of the annual rainfall (Bookhagen and Burbank, 2010). The eastern and western parts of the Himalaya (syntaxes) receive about half of their annual precipitation during the monsoon season; high-elevation regions of the Himalaya, especially in the syntaxes, receive significant precipitation in the form of snow. While this general spatiotemporal pattern is well established (Bookhagen, 2016; 2017), patterns of rainfall trends are less well-studied and generally less reliable due to the short time series and large rainfall heterogeneities in mountainous terrain. Reliable and high-spatial resolution rainfall measurements from satellites started with the TRMM mission (Kummerow et al., 1998) and continue today with the Global Precipitation Measurement Mission (Hue et al., 2014). The ISM exhibits strong decadal and longer-timescale oscillations; trends determined from short timescales do not provide meaningful results for multi-decadal or centennial studies. In order to study multi-decadal trends, researchers often rely on gridded and aggregated rain-gauge data (e.g. APHRODITE). In a recent study, Malik et al. (2016) provide a comprehensive analysis of trends in the extremes during the ISM season. Their analysis, based on quantile regression and gridded rainfall-station data, shows that different regions in India and the Himalaya have divergent and partially opposing rainfall trends. These trends show intensified droughts in Northwest India, parts of Peninsular India, and Myanmar; in contrast, parts of Pakistan, Northwest Himalaya, and Central India show increased extreme daily rain intensity leading to higher flood vulnerability.

Spatial patterns of changes in the Himalayan cryosphere

Spatially and temporally extensive passive microwave SWE estimates can be used to examine decadal trends in snow-water storage throughout the Himalaya. As can be seen in 0, the majority of annual SWE trends are negative throughout the Himalaya, with the exception of parts of the Pamir, the eastern edge of the Tibetan Plateau, and a region along the edge of the Tarim Basin. This implies that over the period 1987 to 2009, less water was stored (on average) in snowpack throughout the Himalaya. To assess the impact of these changes at a watershed scale, we aggregate both SWE volumes and SWE trends across elevations within selected Himalayan catchments to identify regions where changes in SWE will have the strongest downstream effects (0).

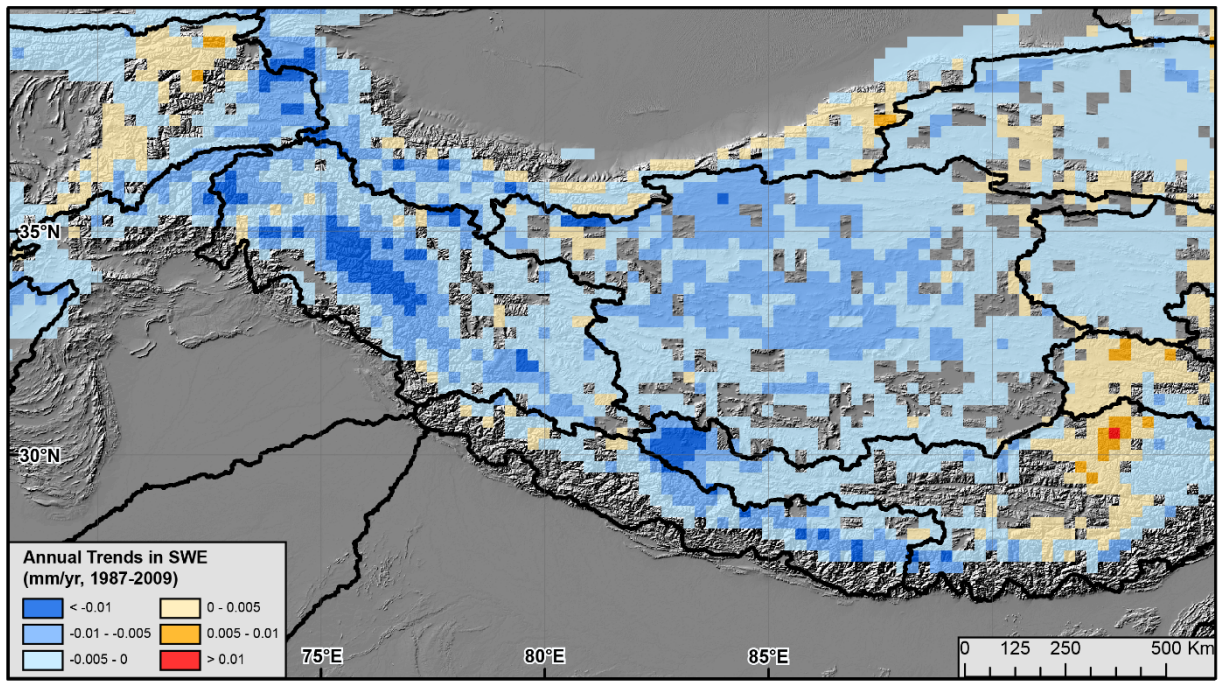


Figure 10 – Annual trends in SWE volume (data derived from SSMI, 1987-2009). While the majority of SWE trends are negative, there exist positive SWE storage trends in the Pamir, parts of the Kunlun Shan, and in parts of Eastern Tibet. Modified from Smith and Bookhagen, 2018.

Across all catchments, there is a strong and non-linear elevation-SWE relationship. In the majority of catchments examined here, the highest-SWE elevation slice occurs below the maximum catchment elevation. The majority of SWE in these catchments is stored in their mid-to-high elevation regions (above 3,500 m asl). These mid-elevation, high-SWE zones also have some of the most negative SWE trends, implying that the negative trends in SWE will likely have a strong impact on downstream water provision. This is in line with increased temperatures in low-precipitation, high-elevation zones of the Himalaya (Bolch et al., 2012; Pepin et al., 2015), and observed changes in Himalayan runoff (Lau et al., 2010; Panday et al., 2011; Lutz et al., 2014).

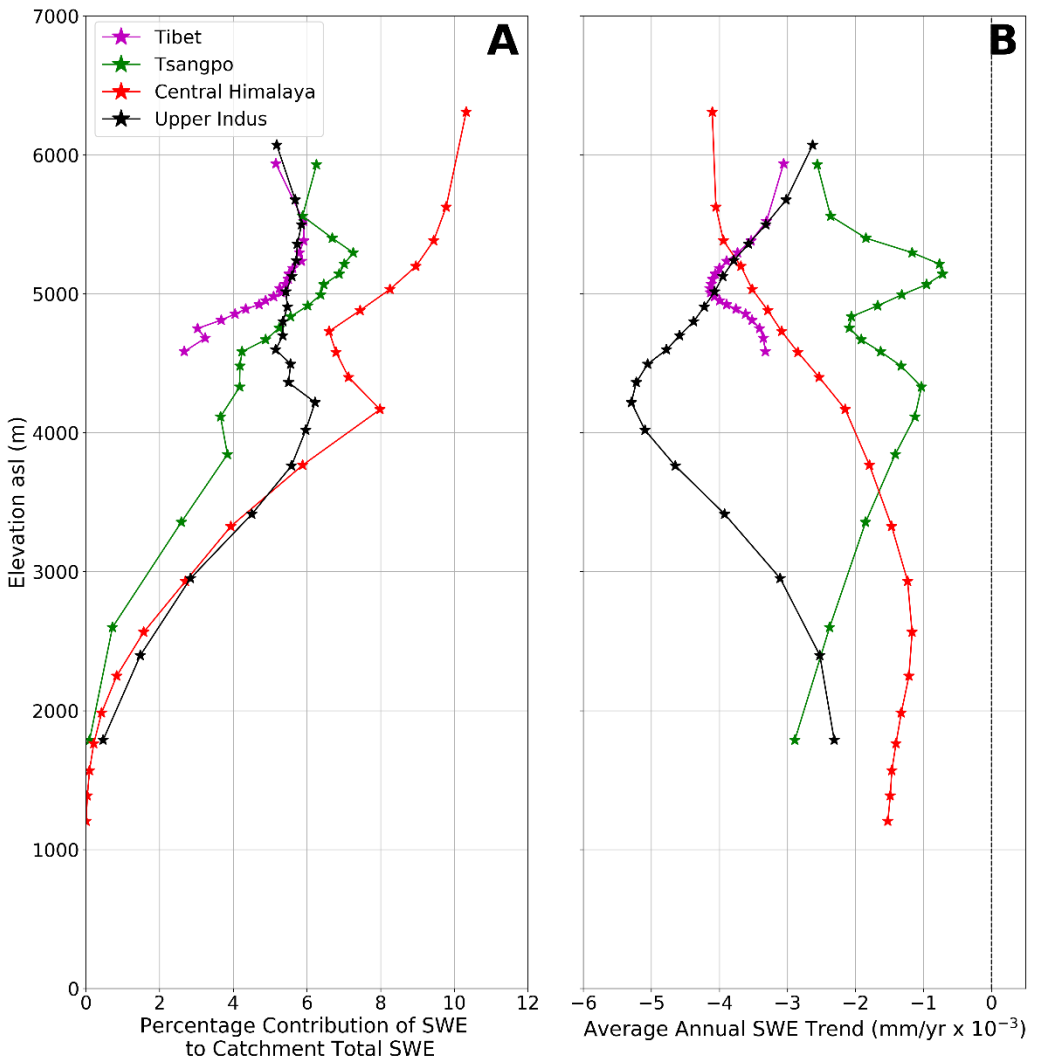


Figure 11 – Elevation SWE relationships. (A) Elevation distribution of SWE in each catchment, at each 5th percentile elevation slice. (B) Average SWE trend at the same 5th percentile elevation slices. SWE trends tend to be the most negative where the highest SWE volumes are stored. This indicates that SWE changes are not just impacting low-elevation, shallow-snow areas, but mostly have impacted medium-elevation zones where there is high SWE storage. See 0 for watershed boundaries. Modified from Smith and Bookhagen, 2018.

In addition to changes in the volume of water stored in snowpack, there have been measurable changes in the timing of the snowmelt season (Smith et al., 2017; Xiong et al., 2017; Panday et al., 2011). In particular, the length of the snowmelt season (time from the onset of the main melt phase until the clearance of snow), has been shrinking over the period 1987 to 2016 (0). The snowmelt season has also tended to both start and end earlier in the year.

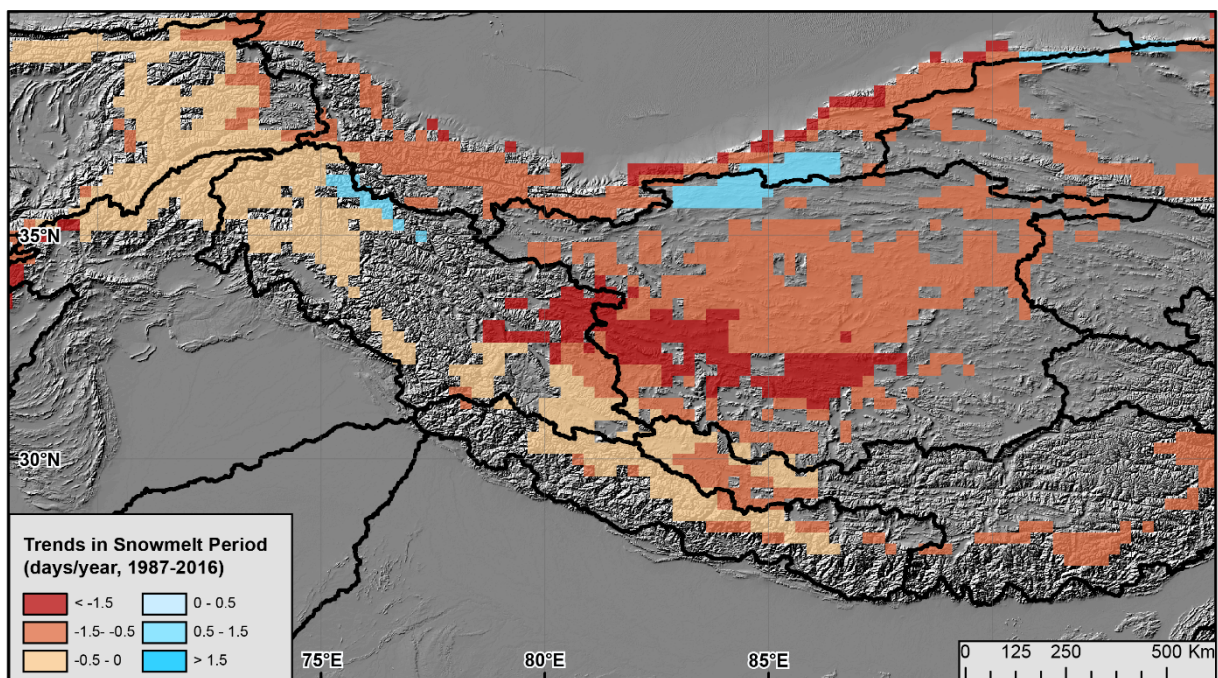


Figure 12 – Trends in snowmelt period (length of time between onset and end of snowmelt), 1987-2016. The majority of the study region has experienced compressed snowmelt seasons over the past decades. Modified from Smith et al., 2017.

Dynamics of snow-water storage and snowmelt

Temperatures in the Himalaya are increasing faster than the global average (Vaughan et al., 2013; Lau et al., 2010). These temperature increases are likely the driver of changes in snow-water storage and snowmelt, due to changes in the timing of snowfall, precipitation phase, and the spatial distribution of precipitation.

There has been an overall decrease in SWE storage in the Himalaya, as well as shifts in the seasonality of SWE buildup and melt (Lau et al., 2010; Panday et al., 2011; Smith and Bookhagen, 2018; Smith et al., 2017). The mechanism behind these SWE changes is not well defined, but likely includes contributions from aerosol contamination (Lau et al., 2010), changes in precipitation phase (Lutz et al., 2014), changes in the strengths of the WWD (Cannon et al., 2014; 2015) and ISM (Singh et al., 2014; Palazzi et al., 2013), and increases in regional temperatures which lead to both more atmospheric water storage and decreased SWE persistence (Vaughan et al., 2013; Yao et al., 2012; Trenberth, 2011). Changes in snowmelt seasonality has been shown to modify downstream water availability (Barnett et al., 2005; Berghuijs et al., 2014).

Glaciers in the Himalaya are generally retreating (Bolch et al., 2012; Gardner et al., 2013; Kääb et al., 2012; 2015); in many cases, retreat is accelerating and small glaciers are disappearing (Armstrong et al., 2010). The reasons behind these changes are multi-faceted and poorly constrained, although debris cover, topography, and precipitation seasonality are factors known to impact glacier stability.

While much of the Himalaya's water budget is monsoon-driven, there exists a precipitation gradient moving west along the front of the Himalaya, where the western reaches of the Himalaya region have a much higher snowmelt and glacier contribution to their water budgets (cf. 0) (Bookhagen and Burbank, 2010). Even in those regions where rainfall is primary, seasonal snowmelt is an important water source for mountain communities and local ecologies.

Snow and glacier melt are primary sources of water at different times of the year; snowmelt generally peaks in the spring before the monsoon, and glacier melt is primary in the post-monsoon season. Both of these segments of the hydrosphere are essential for maintaining consistent and reliable water flow in both natural areas, such as wetlands, and in developed areas, such as hydropower, irrigation, and municipal water systems. Any changes in the temporal distribution of these water resources can increase the frequency of short-term water surpluses and droughts, particularly

in the western and northwestern Himalaya where snow-water resources form a large part of the yearly hydrological budget (Vaughan et al., 2013).

Limitations and caveats of remote-sensing datasets

While remote sensing datasets provide a quasi-continuous and long-term record of earth surface processes, there are several important caveats to consider when interpreting these data records. Each satellite dataset has its own set of strengths and weaknesses which impact the reliability of derived environmental analyses.

TRMM data is limited by its temporal resolution with respect to the often-short duration of precipitation events. In particular, intense monsoonal rainstorms, which account for a significant portion of the regional water budget, are often missed in the gaps between satellite overpasses. In this analysis, we average our high-temporal resolution data to monthly averages to limit the impacts of gaps in the TRMM data record. A second caveat of the TRMM dataset is the well-documented elevation-dependent error, where high-elevation precipitation is underestimated in the region (Bharti and Singh, 2015; Wulf et al., 2016). Thus, precipitation estimates in some of the poorly-monitored, high-elevation regions of the study area should be considered with caution. Furthermore, the low spatial resolution of the TRMM 3B42 datasets (and similar datasets, e.g., APHRODITE) do not capture distinctive orographic rainfall peaks, but provide average measurements for $\sim 25 \times 25$ km areas. Importantly, the previously identified orographic rainfall peak (cf. 0, Bookhagen and Burbank, 2006; Bookhagen and Burbank, 2010) is not well captured in low-resolution TRMM data.

Both MODIS and SPOT data are limited by both the temporal and radiometric resolution of data collection. In much of the study area, long-duration cloud cover and storm systems can prevent optical measurement of earth-surface characteristics for several days at a time. We thus rely on lower temporal resolution products in this study. A second caveat of the MODIS products is the poor performance of LST estimates over snow-covered terrain (Wan, 2008). The MODIS LST algorithm is based on radiation balances, and is adversely impacted by high reflectivity values in the visible and near-infrared spectra over snow.

While passive microwave data provides the most globally extensive means of measuring snow buildup and melt, there are several important sources of error in SWE estimation. The most commonly used SWE estimation algorithms assume that the snowpack is comprised of dry, evenly sized, snow crystals at a constant density. While fresh snow in cold regions often satisfies these conditions, in complex and mountainous terrain, snowpack undergoes progressive metamorphism throughout a given snow season. This changes both the size and density distribution of snowpack, and leads to errors in SWE estimation (Kelly et al., 2003).

There is a well-documented signal saturation in passive microwave data over glaciers and in deep snowpacks (Takala et al., 2011; Tedesco and Narvekar, 2010). As the estimated SWE in a passive microwave pixel is sensitive to the depth of snow throughout the pixel, this saturation can occur even in regions where only a small portion of the pixel overlaps with deep snow (Vander Jagt et al., 2013). In our study area, this mostly impacts glaciated regions, and thus SWE estimates close to glaciers (cf. 0) should be considered more error-prone. A final caveat of passive microwave data is that SWE estimates in the presence of liquid water are highly biased, due to large differences in microwave signal strength between liquid and frozen water. Thus, SWE cannot be estimated near large bodies of water, and SWE estimates during the spring snowmelt season are less reliable than those earlier in the season.

Despite these caveats, passive microwave data remains the only empirical method to estimate SWE over large areas of complex and inhospitable terrain (Chang et al., 1982; 1987; Kelly et al., 2003; Abdalati and Steffen, 1995; Drobot and Anderson, 2001; Takala et al., 2011). The lack of an extensive in-situ sensor network in the region (cf. 0), as well as the difficulties associated with ground-data collection, mean that passive microwave SWE estimates remain the best option for monitoring large-scale snow patterns.

Conclusions

Remote sensing provides the only long-term and spatially-extensive climatic datasets across the diverse terrain of the Himalaya. These data are essential for improving our understanding of environmental changes and our continued prediction of their future magnitudes and impacts. They also provide the basis for calibrating large-scale climate models, which are important tools in predicting the future impacts of climate change.

While remotely sensed data provides valuable insight into large-scale environmental change, the uncertainties in the data must be carefully considered in combination with calibration and field observations – especially when high-resolution datasets are used.

There have already been significant changes to the precipitation regime across the Himalaya, which have impacted not only liquid precipitation but also the buildup and melt of frozen water. Long-term trends indicate a shift towards a shorter and earlier snowmelt season. This has already had, and will continue to have, strong impacts upon both the natural environment and communities which rely on consistency in the volume and timing of snowmelt for year-round water provision. Information on the magnitude and direction of changes will be essential for future water planning.

References

- Abdalati, W. and Steffen, K.: Passive microwave-derived snow melt regions on the Greenland Ice Sheet, *Geophysical Research Letters*, 22, 787–790, 1995.
- Archer, D. R. and Fowler, H.: Spatial and temporal variations in precipitation in the Upper Indus Basin, global teleconnections and hydrological implications, *Hydrology and Earth System Sciences Discussions*, 8, 47–61, 2004.
- Armstrong, R. and Brodzik, M.: Recent Northern Hemisphere snow extent: A comparison of data derived from visible and microwave satellite sensors, *Geophysical Research Letters*, 28, 3673–3676, 2001.
- Armstrong, R. L. et al.: The glaciers of the Hindu Kush-Himalayan region: a summary of the science regarding glacier melt/retreat in the Himalayan, Hindu Kush, Karakoram, Pamir, and Tien Shan mountain ranges., International Centre for Integrated Mountain Development (ICIMOD), 2010.
- Ashcroft, P. and Wentz, F.: AMSR-E/aqua L2A global swath spatially-resampled brightness temperatures V003, [2002–2010]., Boulder, Colorado USA: National Snow and Ice Data Center, 2013.
- Barnett, T. P., Adam, J. C., and Lettenmaier, D. P.: Potential impacts of a warming climate on water availability in snow-dominated regions, *Nature*, 438, 303–309, 2005.
- Berghuijs, W., Woods, R., and Hrachowitz, M.: A precipitation shift from snow towards rain leads to a decrease in streamflow, *Nat. Clim. Change*, 4, 583–586, 2014.
- Bharti, V., and Singh, C.: Evaluation of error in TRMM 3B42V7 precipitation estimates over the Himalayan region, *J. Geophys. Res. Atmos.*, 120, 12458–12473, 2015.
- Bolch, T., Kulkarni, A., Kääb, A., Huggel, C., Paul, F., Cogley, J., Frey, H., Kargel, J., Fujita, K., Scheel, M., et al.: The state and fate of Himalayan glaciers, *Science*, 336, 310–314, 2012.
- Bookhagen, B., Thiede, R. C., and Strecker, M. R.: Abnormal monsoon years and their control on erosion and sediment flux in the high, arid northwest Himalaya, *Earth and Planetary Science Letters*, 231, 131–146, 2005.
- Bookhagen, B., and Burbank, D. W.: Topography, relief, and TRMM-derived rainfall variations along the Himalaya. *Geophysical Research Letters* 33.8, 2006.
- Bookhagen, B. and Burbank, D. W.: Toward a complete Himalayan hydrological budget: Spatiotemporal distribution of snowmelt and rainfall and their impact on river discharge, *Journal of Geophysical Research: Earth Surface* (2003–2012), 115, 2010.
- Bookhagen, B.: Chapter 11: Glaciers and Monsoon Systems, in: *The Monsoons and Climate Change: Observations and Modeling*, edited by Carvalho, L. and Jones, C., Springer Climate, 2016.
- Bookhagen, B.: Chapter 11: The influence of Hydrology and Glaciology on Wetlands in the Himalaya, in: *Bird Migration Across the Himalayas: Wetland Functioning Amidst Mountains and Glaciers*, edited by Prins, H. and Namgail, T., Cambridge University press, 2017.
- Cannon, F., Carvalho, L., Jones, C., and Bookhagen, B.: Multi-annual variations in winter westerly disturbance activity affecting the Himalaya, *Climate Dynamics*, pp. 1–15, 2014.
- Cannon, F., Carvalho, L. M., Jones, C., and Norris, J.: Winter westerly disturbance dynamics and precipitation in the western Himalaya and Karakoram: a wave-tracking approach, *Theoretical and Applied Climatology*, pp. 1–18, 2015.
- Chang, A., Foster, J., Hall, D., Rango, A., and Hartline, B.: Snow water equivalent estimation by microwave radiometry, *Cold Regions Science and Technology*, 5, 259–267, 1982.
- Chang, A., Foster, J., and Hall, D.: Nimbus-7 SMMR derived global snow cover parameters, *Annals of glaciology*, 9, 39–44, 1987.

Dey, S., Thiede, R.C., Schildgen, T.F., Wittmann, H., Bookhagen, B., Scherler, D., Vikrant, J., Strecker, M.R.: Climate-driven sediment aggradation and incision phases since the Late Pleistocene in the NW Himalaya, India, *Earth and Planetary Science Letters*, 449, pp. 321–331, 2016.

Deronde, B., Debruyn, W., Gontier, E., Goor, E., Jacobs, T., Verbeiren, S., and Vereecken, J. 15 years of processing and dissemination of SPOT-VEGETATION products, *International Journal of Remote Sensing*, 35:7, 2402-2420, 2014.

Drobot, S. D. and Anderson, M. R.: An improved method for determining snowmelt onset dates over Arctic sea ice using scanning multichannel microwave radiometer and Special Sensor Microwave/Imager data, 2001.

Frey, H., Machguth, H., Huss, M., Huggel, C., Bajracharya, S., Bolch, T., Kulkarni, A., Linsbauer, A., Salzmann, N., and Stoffel, M.: Estimating the volume of glaciers in the Himalayan–Karakoram region using different methods, *The Cryosphere*, 8, 2313–2333, 2014.

Fu, C.: Potential impacts of human-induced land cover change on East Asia monsoon, *Global and Planetary Change*, 37, 219–229, 2003.

Fujita, K.: Effect of precipitation seasonality on climatic sensitivity of glacier mass balance, *Earth and Planetary Science Letters*, 276, 14–19, 2008.

Fujita, K. and Nuimura, T.: Spatially heterogeneous wastage of Himalayan glaciers, *Proceedings of the National Academy of Sciences*, 108, 14 011–14 014, 2011.

Gardelle, J., Berthier, E., and Arnaud, Y.: Slight mass gain of Karakoram glaciers in the early twenty-first century, *Nature geoscience*, 5, 322–325, 2012.

Gardner, A. S., Moholdt, G., Cogley, J. G., Wouters, B., Arendt, A. A., Wahr, J., Berthier, E., Hock, R., Pfeffer, W. T., Kaser, G., et al.: A reconciled estimate of glacier contributions to sea level rise: 2003 to 2009, *Science*, 340, 852–857, 2013.

Gautam, R., Hsu, N., Lau, K.-M., and Kafatos, M.: Aerosol and rainfall variability over the Indian monsoon region: distributions, trends and coupling, in: *Annales Geophysicae*, vol. 27, pp. 3691–3703, Copernicus GmbH, 2009.

GPM Science Team: GPMGMI Level 1B Brightness Temperatures, version 03, Greenbelt, MD, USA: NASA Goddard Earth Science Data and Information Services Center (GES DISC), 2014.

Hall, D. K., V. V. Salomonson, and G. A. Riggs. 2006. MODIS/Terra Snow Cover Daily L3 Global 0.05Deg CMG, Version 5. Boulder, Colorado USA. NASA National Snow and Ice Data Center Distributed Active Archive Center. doi: <https://doi.org/10.5067/EI5HGLM2NNHN>.

Hirschmiller, J., Grujic, D., Bookhagen, B., Coutand, I., Huyghe, P., Mugnier, J.-L., Ojha, T.: What controls the growth of the Himalayan foreland fold-and-thrust belt? *Geology* ; 42 (3): 247–250, 2014.

Hou, A.Y., R.K. Kakar, S. Neeck, A.A. Azarbarzin, C.D. Kummerow, M. Kojima, R. Oki, K. Nakamura, and T. Iguchi. The Global Precipitation Measurement Mission. *Bull. Amer. Meteor. Soc.*, 95, 701–722, 2014.

Huffman, G. J., Bolvin, D. T., Nelkin, E. J., Wolff, D. B., Adler, R. F., Gu, G., Hong, Y., Bowman, K. P., and Stocker, E. F.: The TRMM multisatellite precipitation analysis (TMPA): Quasi-global, multiyear, combined-sensor precipitation estimates at fine scales, *Journal of Hydrometeorology*, 8, 38–55, 2007.

Imaoka, K., Kachi, M., Kasahara, M., Ito, N., Nakagawa, K., and Oki, T.: Instrument performance and calibration of AMSR-E and AMSR2, *International Archives of the Photogrammetry, Remote Sensing and Spatial Information Science*, 38, 13–18, 2010.

Immerzeel, W. W., Van Beek, L. P., and Bierkens, M. F.: Climate change will affect the Asian water towers, *Science*, 328, 1382–1385, 2010.

Immerzeel, W.W., van Beek, L.P.H., Konz, M. et al. Climatic Change (2012) 110: 721. <https://doi.org/10.1007/s10584-011-0143-4>

Immerzeel, W., Wanders, N., Lutz, A., Shea, J., and Bierkens, M.: Reconciling high-altitude precipitation in the upper Indus basin with glacier mass balances and runoff, *Hydrology and Earth System Sciences*, 19, 4673, 2015.

Jarvis, A., Reuter, H. I., Nelson, A., Guevara, E., et al.: Hole-filled SRTM for the globe Version 4, available from the CGIAR-CSI SRTM 90m Database (<http://srtm.cgiar.org>), 2008.

Kääb, A., Berthier, E., Nuth, C., Gardelle, J., and Arnaud, Y.: Contrasting patterns of early twenty-first-century glacier mass change in the Himalayas, *Nature*, 488, 495–498, 2012.

Kääb, A., Treichler, D., Nuth, C., and Berthier, E.: Brief Communication: Contending estimates of 2003–2008 glacier mass balance over the Pamir–Karakoram–Himalaya, *The Cryosphere*, 9, 557–564, 2015.

Kapnick, S. B., Delworth, T. L., Ashfaq, M., Malyshev, S., and Milly, P.: Snowfall less sensitive to warming in Karakoram than in Himalayas due to a unique seasonal cycle, *Nature Geoscience*, 7, 834–840, 2014.

Kelly, R. E., Chang, A. T., Tsang, L., and Foster, J. L.: A prototype AMSR-E global snow area and snow depth algorithm, *Geoscience and Remote Sensing, IEEE Transactions*, 41, 230–242, 2003.

Kitoh, A., Endo, H., Krishna Kumar, K., Cavalcanti, I. F., Goswami, P., and Zhou, T.: Monsoons in a changing world: a regional perspective in a global context, *Journal of Geophysical Research: Atmospheres*, 118, 3053–3065, 2013.

Kummerow C, Barnes W, Kozu T, Shiue J, Simpson J. The tropical rainfall measuring mission (TRMM) sensor package. *Journal of atmospheric and oceanic technology*, 15(3):809-17, 1998.

Lau, W. K., Kim, M.-K., Kim, K.-M., and Lee, W.-S.: Enhanced surface warming and accelerated snow melt in the Himalayas and Tibetan Plateau induced by absorbing aerosols, *Environmental Research Letters*, 5, 025 204, 2010.

Li, L., Gochis, D. J., Sobolowski, S., and Mesquita, M. d. S.: Evaluating the present annual water budget of a Himalayan headwater river basin using a high-resolution atmosphere-hydrology model, *Journal of Geophysical Research: Atmospheres*, 2017.

Lutz, A., Immerzeel, W., Shrestha, A., and Bierkens, M.: Consistent increase in High Asia's runoff due to increasing glacier melt and precipitation, *Nature Climate Change*, 4, 587–592, 2014.

Malik, N., Bookhagen, B., and Mucha, P. J.: Spatiotemporal patterns and trends of Indian monsoonal rainfall extremes, *Geophysical Research Letters*, 43, 1710–1717, 2016.

Maussion, F., Scherer, D., Mölg, T., Collier, E., Curio, J., and Finkelburg, R.: Precipitation Seasonality and Variability over the Tibetan Plateau as Resolved by the High Asia Reanalysis, *Journal of Climate*, 27, 1910–1927, 2014.

Menon, A., Levermann, A., and Schewe, J.: Enhanced future variability during India's rainy season, *Geophysical Research Letters*, 40, 3242–3247, 2013.

Palazzi, E., Hardenberg, J., and Provenzale, A.: Precipitation in the Hindu-Kush Karakoram Himalaya: Observations and future scenarios, *Journal of Geophysical Research: Atmospheres*, 118, 85–100, 2013.

Olen, S.M., Bookhagen, B., and Strecker, M.R.: Role of climate and vegetation density in modulating denudation rates in the Himalaya, *Earth and Planetary Science Letters*, Volume 445, p. 57-67, 2016.

Panday, P. K., Frey, K. E., and Ghimire, B.: Detection of the timing and duration of snowmelt in the Hindu Kush-Himalaya using QuikSCAT, 2000–2008, *Environmental Research Letters*, 6, 024 007, 2011.

Pepin, N., Bradley, R. S., Diaz, H. F., Baraer, M., Caceres, E. B., Forsythe, N., Fowler, H., Greenwood, G., Hashmi, M. Z., Liu, X. D., Miller, J. R., Ning, L., Ohmura, A., Palazzi, E., Rangwala, I., Schöner, W., Severskiy, I., Shahgedanova, M., Wang, M. B., Williamson, S. N., and Yang, D. Q.: Elevation-dependent warming in mountain regions of the world, *Nature Climate Change*, 5, 424–430, 2015.

Ramanathan, V., Chung, C., Kim, D., Bettge, T., Buja, L., Kiehl, J., Washington, W., Fu, Q., Sikka, D., and Wild, M.: Atmospheric brown clouds: Impacts on South Asian climate and hydrological cycle, *Proceedings of the National Academy of Sciences of the United States of America*, 102, 5326–5333, 2005.

RGI Consortium. Randolph Glacier Inventory – A Dataset of Global Glacier Outlines: Version 6.0; Technical Report, Global Land Ice Measurements from Space, Colorado, USA. Digital Media, 2017. DOI: <https://doi.org/10.7265/N5-RGI-60>

Scherler, D., Bookhagen, B., and Strecker, M. R.: Spatially variable response of Himalayan glaciers to climate change affected by debris cover, *Nature Geoscience*, 4, 156–159, 2011.

Singh, D., Tsiang, M., Rajaratnam, B., and Diffenbaugh, N. S.: Observed changes in extreme wet and dry spells during the South Asian summer monsoon season, *Nature Climate Change*, 4, 456–461, 2014.

Smith, T., and Bookhagen, B.: Assessing uncertainty and sensor biases in passive microwave data across High Mountain Asia, *Remote Sensing of the Environment*, Volume 181, Pages 174-185, 2016.

Smith, T., Bookhagen, B., and Rheinwald, A.: Spatiotemporal Patterns of High Mountain Asia's Snowmelt Season Identified with an Automated Snowmelt Detection Algorithm, 1987–2016, *The Cryosphere*, 2017.

Smith, T., and Bookhagen, B.: Changes in seasonal snow- water equivalent distribution in High Mountain Asia (1987 to 2009), *Science Advances* 4: 1, 2018.

Sorg, A., Bolch, T., Stoffel, M., Solomina, O., and Beniston, M.: Climate change impacts on glaciers and runoff in Tien Shan (Central Asia), *Nature Climate Change*, 2, 725–731, 2012.

Sun, N. and Weng, F.: Evaluation of special sensor microwave imager/sounder (SSMIS) environmental data records, *Geoscience and Remote Sensing, IEEE Transactions*, 46, 1006–1016, 2008.

Takala, M., Luojus, K., Pulliainen, J., Derksen, C., Lemmetyinen, J., Kärnä, J.-P., Koskinen, J., and Bojkov, B.: Estimating northern hemisphere snow water equivalent for climate research through assimilation of space-borne radiometer data and ground-based measurements, *Remote Sensing of Environment*, 115, 3517–3529, 2011.

Tedesco, M. and Narvekar, P. S.: Assessment of the NASA AMSR-E SWE Product, *Selected Topics in Applied Earth Observations and Remote Sensing, IEEE Journal of*, 3, 141–159, 2010.

Thiede, R. C., T. A. Ehlers, B. Bookhagen, and M. R. Strecker (2009), Erosional variability along the northwest Himalaya, *J. Geophys. Res.*, 114, F01015, doi: 10.1029/2008JF001010.

Trenberth, K. E.: Changes in precipitation with climate change, *Climate Research*, 47, 123–138, 2011.

Vander Jagt, B. J., Durand, M. T., Margulis, S. A., Kim, E. J., and Molotch, N. P.: The effect of spatial variability on the sensitivity of passive microwave measurements to snow water equivalent, *Remote Sensing of Environment*, 136, 163–179, 2013.

Vaughan, D., Comiso, J., Allison, I., Carrasco, J., Kaser, G., Kwok, R., Mote, P., Murray, T., Paul, F., Ren, J., Rignot, E., Solomina, O., Steffen, K., and Zhang, T.: Observations: Cryosphere. In: *Climate Change 2013: The Physical Science Basis., Contribution of Working Group I to the Fifth Assessment Report of the IPCC.*, 2013.

Wan, Z.: New refinements and validation of the MODIS land-surface temperature/emissivity products. *Remote sensing of Environment* 112.1: 59-74, 2008.

Wan, Z., S. Hook, G. Hulley. MOD11A2 MODIS/Terra Land Surface Temperature/Emissivity 8-Day L3 Global 1km SIN Grid V006. 2015.

Wentz, F. J.: SSM/I version-7 calibration report, *Remote Sensing Systems Rep*, 11012, 46, 2013.

Wulf, H., Bookhagen, B., and Scherler, D.: Differentiating between rain, snow, and glacier contributions to river discharge in the western Himalaya using remote-sensing data and distributed hydrological modeling, *Advances in Water Resources*, 88, 152–169, 2016.

Xiong, C., Shi, J., Cui, Y., and Peng, B.: Snowmelt Pattern Over High-Mountain Asia Detected From Active and Passive Microwave Remote Sensing, *IEEE Geoscience and Remote Sensing Letters*, 2017.

Yao, T., Thompson, L., Yang, W., Yu, W., Gao, Y., Guo, X., Yang, X., Duan, K., Zhao, H., Xu, B., et al.: Different glacier status with atmospheric circulations in Tibetan Plateau and surroundings, *Nature Climate Change*, 2, 663–667, 2012.

Yatagai, A., Kamiguchi, K., Arakawa, O., Hamada, A., Yasutomi, N., and Kitoh, A.: APHRODITE: Constructing a long-term daily gridded precipitation dataset for Asia based on a dense network of rain gauges, *Bulletin of the American Meteorological Society*, 93, 1401–1415, 2012.